

Crystal chemistry of the dravite–chromdravite series

Ferdinando Bosi^{1,*}, Sergio Lucchesi^{1,**} and Leonid Reznitskii^{2,***}

¹Dipartimento di Scienze della Terra, Università di Roma “La Sapienza”, P.le A. Moro 5, 00185 Roma, Italy.

²Russian Academy of Science. Siberian Branch, Institute of the Earth’s crust, Lermontova str., 128, Irkutsk, Russia.

Abstract: Five Cr-dravite–chromdravite samples, representative of the high-chromium part of the compositional field observed in tourmalines occurring in rocks surrounding Lake Baikal, were selected and studied by electron microprobe analysis and structural refinement. All examined tourmalines belong to the *Alkali group, Oxy-subgroup*. Their most striking feature is the exceptionally high Cr content (from 3.2 to 4.41 apfu), which substitutes for Al. The main divalent cation is Mg. Site populations were determined by a minimization procedure which simultaneously takes into account both structural and chemical data. Empirical bond distances for ${}^Y\text{Cr}^{3+}\text{-O}$ (1.978 Å) and ${}^Z\text{Cr}^{3+}\text{-O}$ (1.970 Å) were optimised within the minimization procedure. Results indicate that the crystals are characterized by a quite disordered cation distribution between *Y* and *Z* octahedral sites, the various cations showing different degrees of preference. Cr^{3+} and Mg populate both sites but show opposite behaviour: Mg has a marked preference for the *Z* octahedron and Cr^{3+} for *Y*. Al almost exclusively populates *Z*. Most structural features are related to variations in the *Z* octahedron, whereas the dimensions of other polyhedra remain almost constant. *Z* dimensions depend on site populations, and are in particular determined by the ${}^Z\text{Cr}^{3+} \leftrightarrow {}^Z\text{Al}$ substitution.

In the dravite–chromdravite series, both current and literature data show that the unit cell parameter *c* is strongly and positively correlated with *Z* dimensions, while correlation with *a* is evident only within the Cr-dravite–chromdravite subseries. *Y* does not actively participate in structural variations and, in particular, no correlation was ever observed between *Y* dimensions and unit cell parameters. Most structural variations are thus due to *Z*, while the effects of *Y* are negligible. This behaviour stands out when examining the *a* vs. *c* plot, for the whole series: a strong correlation between the two unit cell parameters was observed in the Cr-dravite–chromdravite subseries, but none within the dravite–Cr-dravite subseries or schorl–dravite series.

Key-words: crystal structure, crystal chemistry, tourmaline, chromdravite, disorder.

Introduction

The structure of tourmaline is characterized by remarkable flexibility (Foit, 1989) and this feature results in a wide spectrum of constituent cations. This complex crystal chemistry, further complicated by extensive intracrystalline disorder, may be appreciated when examining the general formula and all the possible site populations: $XY_3Z_6[T_6O_{18}](BO_3)_3V_3W$, where: *X* = Ca, Na, K, □; *Y* = Li, Mg, Fe^{2+} , Mn^{2+} , Zn, Al, Cr^{3+} , V^{3+} , Fe^{3+} , Ti^{4+} ; *Z* = Mg, Al, Fe^{2+} , Fe^{3+} , Cr^{3+} , V^{3+} ; *T* = Si, Al, B; *B* = B, □; *V* = OH, O; *W* = OH, F, O. Although most tourmaline findings are restricted to the schorl–dravite–elbaite range, “exotic” compositions are not rare, and cations which are usually in low concentrations may reach significant contents: chromium is among such cations. Chromium-rich tourmalines were already described in the 19th century (Cossa & Arzruni, 1883) and are nowadays known in many regions throughout the world, in a variety of geological settings. Chromdravite, a new mineral species containing Cr^{3+} as major constituent, was discovered in 1983 in Karelia, Russia (Rumyantseva, 1983). A few years

later, chromdravite and tourmalines of the dravite–chromdravite series were found in metamorphic rocks of the Sludyanka crystalline complex, on the southern shore of Lake Baikal (Reznitskii *et al.*, 1988). The chromdravite localities of Karelia and Sludyanka are unique areas of the chromdravite occurrence in the world so far.

Earlier crystal chemical studies on Cr-tourmalines are very sparse (Nuber & Schmetzer, 1979, and references therein) and their structural formula posed many problems (Foit, 1989). However, recently Gorskaya *et al.* (1984) published some structural data for chromdravite in which most Cr^{3+} was located in the *Z* site. These tourmalines were also characterized by significant amounts of Fe. Instead, Sludyanka Cr-tourmalines (Reznitskii *et al.*, 1988) contain virtually no Fe (0.00–0.15 apfu) and are characterized by stable concentrations of Mg (1.9–2.3 apfu), and variable components (Al, Cr^{3+} and V^{3+}) form strict negative correlations between Al and Cr or Al and (Cr + V). So the Sludyanka tourmalines provide the possibility of investigating pure dravite–chromdravite series in which $\text{Cr}^{3+} \leftrightarrow \text{Al}^{3+}$ substitution is the only possible one.

*E-mail: ferdinando.bosi@uniroma1.it; **sergio.lucchesi@uniroma1.it; ***garry@crust.irk.ru

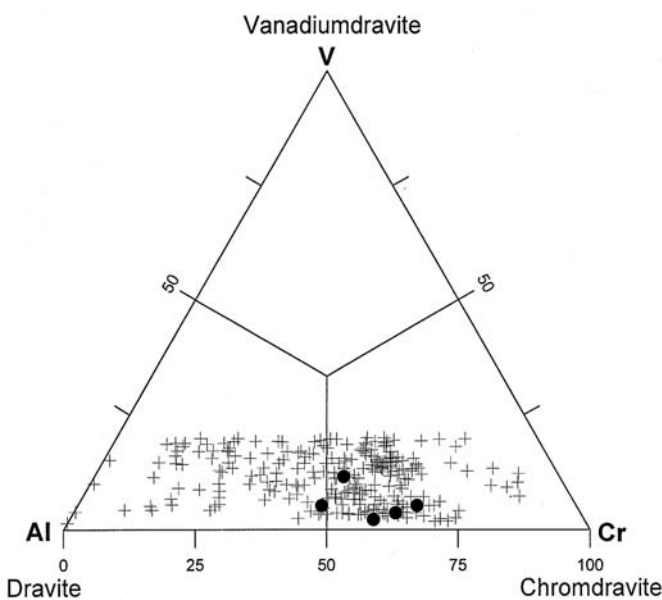


Fig. 1. Al-Cr-V ternary diagram for dravite–chromdravite series from Sludyanka rocks. Full circles: composition of tourmalines studied in the present paper.

Study of the chromdravite end-member is not only useful for clarifying the behaviour of Cr^{3+} but may also help in understanding the main structural relationships of tourmaline. This paper presents results on the chromium-rich part of the Al-Cr series, *i.e.* Cr-dravite–chromdravite, also in comparison with literature data on Cr-bearing ($\text{Cr} > 0.1$ apfu) tourmalines (Foit & Rosenberg, 1979; Gorskaya *et al.*, 1984; Bosi, 2001; Bosi & Lucchesi, 2004).

Occurrence of Cr-tourmaline

The Sludyanka crystalline complex (southern shore of Lake Baikal, Russia) is one of the high-grade metamorphic terrains of the Central Asian mobile belt. The complex includes sequences of interlayered gneisses, crystalline shists, marbles and carbonate-silicate rocks metamorphosed in granulite facies at 480–485 Ma (Salnikova *et al.*, 1998). One of the typical lithologic sequences is the so-called quartz-diopside rock suite, which is derived from siliceous-dolomitic sediments. This suite includes several rock types differing by quantitative ratios of three main rock-forming minerals (quartz, diopside, calcite) from essentially diopside rocks (diopsidite), diopside-bearing and quartz-diopside-bearing calciphyre to quartz-diopside rocks and quartzite. The metamorphogenic chromium-vanadium mineralization is represented by a wide spectrum of Cr-V opaque and silicate minerals, irregularly distributed throughout the rock varieties of the suite (Reznitskii & Sklyarov, 1996). Accessory tourmalines occur in quartz-bearing rocks and form inclusions of euhedral and subhedral prismatic crystals up to 0.3–0.8 mm in quartz. Tourmalines make up complete ternary Al-V-Cr series of dravite–chromdravite–vanadiumdravite solid

Table 1. Parameters for X-ray data collection.

Determination of unit cell parameters	
Radiation	Mo- $K\alpha_1$ (0.70930 Å)
Reflections used	13 (Friedel pairs on both +2 θ and -2 θ)
Range	85° – 95° 2 θ
Temperature	296 K
Diffraction intensity collection	
Radiation	Mo- $K\alpha$ (0.71073 Å)
Monochromator	High crystallinity graphite crystal
Range	3° – 70° 2 θ
Reciprocal space range	0 ≤ h , k ≤ 26 -12 ≤ l ≤ 12
Scan method	ω
Scan range	2.4° 2 θ
Scan speed	Variable 2.93° – 29.30° 2 θ /min
Temperature	296 K
Data reduction	
Refinement	SHELXTL – PC
Corrections	Lorentz, Polarization
Absorption correction	Semi-empirical, 13 Ψ scans (10° – 95° 2 θ)

solutions (Reznitskii *et al.*, 2001). Within the framework of the series, crystals of binary Cr-V, Al-V and Al-Cr series were also found. The most vanadium-poor tourmalines of the dravite–chromdravite series coexist in some types of mica-bearing quartzites, in paragenesis with chromphyllite and other chromium-rich minerals such as escaolaite, chromite, uvarovite, Cr-phlogopite and pyroxenes of the diopside-kosmochlor series (Reznitskii *et al.*, 1997).

Experimental

X-ray diffraction and structural analysis

Five Cr-dravite–chromdravite samples were selected, representative of the high-chromium part of the compositional field observed in tourmalines occurring in rocks surrounding Lake Baikal (Fig. 1). Crystals were crushed, and suitable equidimensional fragments (~0.2 mm) were hand-picked, cemented on glass capillaries, and mounted on a Siemens P4 four-circle single-crystal automated diffractometer for X-ray diffraction study (Table 1). Cell parameters (Table 2) were measured using 52 reflections (13 independent and their Friedel pairs, on both sides of the direct beam). Scan speed varied, depending on reflection intensity, estimated with a pre-scan. Background was measured with a stationary crystal and counter at the beginning and end of each scan, in both cases for half the scan time. Three standard reflections were monitored every 47 measurements. Preliminary full reciprocal space exploration was accomplished: no violations of $R3m$ symmetry were noted.

Data reduction and structural refinement were performed with the SHELXTL-PC program package furnished by Siemens Analytical, X-ray Instruments, Inc.

Table 2. Data collection and refinement information for the crystals studied.

Sample	a (Å)	c (Å)	# refl.	EXT.	R _{all} (%)
TMt3b	16.0539(7)	7.3247(5)	1748	0.00042(2)	1.69
TMt6b	16.0377(8)	7.3157(5)	1740	0.00021(2)	1.83
TMt3c	16.0299(7)	7.3056(5)	1729	0.00030(3)	2.02
TMpr79f	16.0204(11)	7.2985(8)	1728	0.00016(2)	1.83
TM1p43e	15.9911(14)	7.2764(9)	1718	0.00011(2)	1.85

Notes: # refl. = number of observed independent reflections; EXT. = Isotropic secondary extinction coefficient; R_{all} in the form: $(\sum |F_{obs} - F_{calc}|) / (\sum F_{obs})$.

X-ray diffraction intensities were initially corrected for Lorentz and polarization effects. Absorption correction was performed using a semi-empirical method (Table 1). Reflections with $I > 2(\sigma)$ were used (Table 2) from the original set of 1862–1829 data, in a full-matrix least-squares refinement, with unitary weights, in space group *R3m*. Absolute configuration was evaluated according to Barton (1969) and starting coordinates were taken from Foit (1989). The scale factor, isotropic secondary extinction coefficient, atomic coordinates, mean atomic numbers (m.a.n.) of X, Y, Z, and T sites, and displacement factors were variable parameters. No chemical constraints were applied during refinement. Scattering curves for neutral B, partially ionised Si, Al, Cr and O, and fully ionised Mg and Na were used because they proved to furnish the best values of conventional agreement factors over all $\sin\theta/\lambda$ intervals. This combination also gave satisfactory agreement between values of total m.a.n. obtained by structural refinement and electron microprobe analysis (within 1σ of the latter). Three cycles of isotropic refinement were followed by anisotropic cycles until convergence to satisfactory *R* values (1.69–2.02 %; Table 2). Atomic coordinates and displacement factors are shown in Table 3. Selected interatomic distances, polyhedral volumes, polyhedral distortion $\langle\lambda\rangle$ (Robinson *et al.*, 1971) and m.a.n. are listed in Table 4.

Chemical analysis

After X-ray data collection, the structure crystals were mounted on glass slides, polished and carbon-coated for electron microprobe analysis (WDS-EDS method) on a CAMECA CX827 instrument, operating at an accelerating potential of 15 kV and a sample current of 15 nA. For raw data reduction, ZAF and PAP (Pouchou & Pichoir, 1984) programs were applied. The following natural and synthetic standards were used: anorthite (Al), rutile (Ti), olivine (Si, Fe), rhodonite (Mn), diopside (Mg, Ca), sphalerite (Zn), orthoclase (Na, K), fluorite (F) and synthetic metals (Cr, V). No less than 10 point analyses were performed for each specimen. All iron was calculated as Fe²⁺. Each element determination (Table 5) was accepted after checking that the ratio between intensity of the analysed standard before and after each determination was within 1.00 ± 0.01 . Precision for major elements (Al, Cr, Mg, Si) is within ~ 1% of the actual amount present; that for minor elements is within ~ 5 %.

Table 3. Atomic coordinates and displacement parameters ($\times 10^4 \text{ \AA}^2$) for the crystals studied.

Atom	TMt3b	TMt6b	TMt3c	TMpr79f	TM1p43e	
X	x	0	0	0	0	
	y	0	0	0	0	
	z	0.2255(2)	0.2254(3)	0.2237(3)	0.2251(2)	0.2245(2)
U _{eq}	0.0171(4)	0.0183(5)	0.0186(6)	0.0179(5)	0.0180(5)	
Y	x	0.12335(2)	0.12339(2)	0.12337(3)	0.12337(2)	0.12349(2)
	y	½ x	½ x	½ x	½ x	½ x
	z	0.63774(6)	0.63757(7)	0.63710(8)	0.63729(6)	0.63680(6)
U _{eq}	0.00408(9)	0.0045(1)	0.0045(1)	0.0044(1)	0.0045(1)	
Z	x	0.29779(2)	0.29781(2)	0.29791(3)	0.29783(2)	0.29794(2)
	y	0.26179(2)	0.26188(2)	0.26194(3)	0.26189(2)	0.26194(2)
	z	0.60896(6)	0.60891(7)	0.60892(8)	0.60889(7)	0.60929(7)
U _{eq}	0.0045(1)	0.0052(1)	0.0055(1)	0.0053(1)	0.0054(1)	
B	x	0.10977(7)	0.10992(8)	0.1100(1)	0.10995(8)	0.11011(7)
	y	2x	2x	2x	2x	2x
	z	0.4543(3)	0.4541(3)	0.4543(4)	0.4542(3)	0.4541(3)
U _{eq}	0.0045(6)	0.0048(7)	0.0054(8)	0.0049(6)	0.0047(6)	
T	x	0.19001(2)	0.19013(3)	0.19027(3)	0.19032(2)	0.19050(2)
	y	0.18832(2)	0.18840(3)	0.18858(3)	0.18856(3)	0.18872(3)
	z	0	0	0	0	0
U _{eq}	0.0041(1)	0.0046(1)	0.0040(2)	0.0043(1)	0.0044(1)	
O1	x	0	0	0	0	
	y	0	0	0	0	
	z	0.7652(3)	0.7651(4)	0.7654(4)	0.7653(3)	0.7653(3)
U _{eq}	0.0054(5)	0.0067(5)	0.0062(6)	0.0060(5)	0.0064(5)	
O2	x	0.06021(5)	0.06024(5)	0.06041(6)	0.06030(5)	0.06044(5)
	y	2x	2x	2x	2x	2x
	z	0.4891(2)	0.4893(2)	0.4887(3)	0.4882(2)	0.4883(2)
U _{eq}	0.0059(4)	0.0064(4)	0.0068(5)	0.0064(4)	0.0067(4)	
O3	x	0.2564(1)	0.2565(1)	0.2570(1)	0.2569(1)	0.2577(1)
	y	½ x	½ x	½ x	½ x	½ x
	z	0.5098(2)	0.5102(2)	0.5097(3)	0.5098(2)	0.5099(2)
U _{eq}	0.0088(4)	0.0097(4)	0.0100(5)	0.0092(4)	0.0100(4)	
O4	x	0.09250(5)	0.09262(6)	0.09276(7)	0.09258(6)	0.09270(6)
	y	2x	2x	2x	2x	2x
	z	0.0717(2)	0.0720(2)	0.0718(3)	0.0717(2)	0.0716(2)
U _{eq}	0.0090(4)	0.0100(4)	0.0098(5)	0.0092(4)	0.0098(4)	
O5	x	0.1824(1)	0.1826(1)	0.1829(1)	0.1827(1)	0.1832(1)
	y	½ x	½ x	½ x	½ x	½ x
	z	0.0913(2)	0.0913(2)	0.0918(2)	0.0916(2)	0.0916(2)
U _{eq}	0.0086(4)	0.0089(4)	0.0088(5)	0.0086(4)	0.0087(4)	
O6	x	0.19138(7)	0.19144(8)	0.19186(9)	0.19182(7)	0.19234(7)
	y	0.18214(7)	0.18221(8)	0.18238(9)	0.18237(7)	0.18293(7)
	z	0.7802(1)	0.7803(2)	0.7793(2)	0.7796(1)	0.7791(1)
U _{eq}	0.0063(3)	0.0074(3)	0.0073(4)	0.0068(3)	0.0070(3)	
O7	x	0.28320(7)	0.28310(8)	0.28339(9)	0.28347(7)	0.28368(7)
	y	0.28263(7)	0.28278(7)	0.28328(9)	0.28306(7)	0.28345(7)
	z	0.0737(1)	0.0734(2)	0.0737(2)	0.0737(2)	0.0744(1)
U _{eq}	0.0081(3)	0.0091(3)	0.0087(4)	0.0086(3)	0.0089(3)	
O8	x	0.20739(7)	0.20752(8)	0.20787(9)	0.20776(7)	0.20809(7)
	y	0.26778(7)	0.26819(8)	0.26860(9)	0.26828(7)	0.26881(7)
	z	0.4377(2)	0.4382(2)	0.4380(2)	0.4383(2)	0.4384(2)
U _{eq}	0.0093(3)	0.0104(4)	0.0103(4)	0.0098(3)	0.0101(3)	
H3	x	0.259(5)	0.237(5)		0.248(3)	0.252(5)
	y	½ x	½ x		½ x	½ x
	z	0.39(1)	0.36(1)		0.382(7)	0.38(1)
U _{eq}	0.14(3)	0.14(3)		0.07(2)	0.15(3)	

Chemical composition

Chemical composition assessment

According to recent investigations in Mg-poor tourmalines, boron may be > 3 apfu with excess in the *T* site (Hughes *et al.*, 2001). In the present case, this hypothesis was discarded on the basis of the observed *T* structural parameters (m.a.n. and $\langle T-O \rangle$), both consistent with ^{IV}Si \leftrightarrow ^{IV}Al substitution. Also boron deficiency has been discarded since the mean bond distance, $\langle\langle B-O \rangle\rangle =$

Table 4. Bond distances (Å), polyhedral volumes V (Å³), polyhedral distortions <λ> and m.a.n. for the crystals studied.

Sample	TMt3b	TMt6b	TMt3c	TMpr79f	TM1p43e
Site B					
B-O2	1.401(3)	1.404(3)	1.400(3)	1.400(3)	1.398(3)
B-O8A x 2	1.363(1)	1.361(1)	1.364(2)	1.362(1)	1.362(1)
<B-O>	1.376	1.375	1.376	1.375	1.374
m.a.n. B	5	5	5	5	5
Site T					
T-O4	1.6265(5)	1.6268(6)	1.6259(6)	1.6259(5)	1.6240(5)
T-O5	1.644(1)	1.643(1)	1.644(1)	1.642(1)	1.640(1)
T-O7	1.5989(9)	1.595(1)	1.599(1)	1.597(1)	1.597(1)
T-O6	1.614(1)	1.611(1)	1.616(1)	1.6126(9)	1.611(1)
<T-O>	1.621	1.619	1.621	1.619	1.618
V _T	2.177(3)	2.170(3)	2.180(4)	2.171(2)	2.166(3)
<λ _T >	1.0026	1.0025	1.0024	1.0026	1.0024
m.a.n. T	13.99(6)	13.87(6)	13.80(7)	14.05(6)	13.96(5)
Site X					
X-O2B,F x 3	2.556(2)	2.555(2)	2.562(2)	2.547(2)	2.547(2)
X-O4B,F x 3	2.808(1)	2.807(1)	2.804(2)	2.802(1)	2.798(1)
X-O5B,F x 3	2.720(1)	2.719(1)	2.716(2)	2.716(1)	2.715(1)
<X-O>	2.694	2.693	2.694	2.688	2.687
V _X	32.46(1)	32.40(1)	32.44(1)	32.23(1)	32.17(1)
m.a.n. X	12.1(1)	11.4(1)	11.6(1)	12.0(1)	11.7(1)
Site Y					
Y-O1	1.953(1)	1.951(1)	1.952(1)	1.9499(8)	1.949(1)
Y-O2B x 2	2.015(1)	2.012(1)	2.012(2)	2.012(1)	2.008(1)
Y-O3	2.074(1)	2.070(1)	2.075(2)	2.073(1)	2.075(1)
Y-O6C x 2	1.9771(8)	1.9767(9)	1.976(1)	1.9746(9)	1.9765(9)
<Y-O>	2.002	2.000	2.001	1.999	1.999
V _Y	10.416(6)	10.382(6)	10.391(7)	10.375(5)	10.352(5)
<λ _Y >	1.0180	1.0182	1.0186	1.0185	1.0194
m.a.n. Y	22.4(1)	22.3(2)	22.2(2)	22.2(1)	21.3(1)
Site Z					
Z-O3	2.0356(9)	2.033(1)	2.032(1)	2.030(1)	2.024(1)
Z-O6	1.985(1)	1.984(1)	1.974(1)	1.9738(9)	1.960(1)
Z-O8	1.9566(9)	1.953(1)	1.952(1)	1.9471(9)	1.944(1)
Z-O7E	1.960(1)	1.957(1)	1.948(1)	1.950(1)	1.939(1)
Z-O7D	1.990(1)	1.986(1)	1.981(1)	1.980(1)	1.973(1)
Z-O8E	1.9455(9)	1.942(1)	1.934(1)	1.9375(9)	1.9254(9)
<Z-O>	1.979	1.976	1.970	1.970	1.961
V _Z	10.107(5)	10.063(4)	9.972(6)	9.968(4)	9.838(4)
<λ _Z >	1.0150	1.0149	1.0152	1.0151	1.0150
m.a.n. Z	16.73(8)	16.02(9)	15.80(9)	15.66(7)	15.12(7)

1.375(1) Å, is that observed for B in planar triangular coordination both in inorganic structures and in tourmaline (Hawthorne *et al.*, 1996; Pieczka, 1999). As a consequence, B was considered stoichiometric.

As OH turned out to be the only variable, its contents could be calculated on the basis of charge balance requirements.

According to Hawthorne & Henry's (1999) classification, all examined tourmalines belong to the *Alkali group*. Regarding the *W* site, samples fall within the *Oxy-subgroup* (¹⁸O content ranges from 0.61 to 0.74 apfu; F does not

Table 5. Chemical composition (wt. %) of the crystals studied.

Sample	TMt3b	TMt6b	TMt3c	TMpr79f	TM1p43e
SiO ₂	32.5(3)	33.0(3)	33.1(3)	33.6(5)	33.3(3)
TiO ₂	0.03(1)	0.24(5)	0.02(2)	0.23(3)	0.02(2)
B ₂ O ₃	9.6(5)	9.8(5)	9.9(5)	9.8(5)	9.7(5)
Al ₂ O ₃	9.7(3)	11.4(7)	14.0(4)	13(1)	15.9(4)
Cr ₂ O ₃	30.9(4)	30(1)	24.2(6)	28(1)	22.7(9)
V ₂ O ₃	2.5(2)	1.7(3)	5.8(5)	1.03(8)	2.5(3)
FeO _{tot.}	0.32(6)	0.21(6)	0.15(9)	0.2(1)	0.21(9)
MnO	–	–	–	–	–
MgO	8.33(8)	8.4(2)	7.8(3)	8.3(2)	8.1(1)
ZnO	0.13(7)	0.00	0.05(5)	0.06(6)	0.09(6)
CaO	0.38(3)	0.35(8)	0.2(1)	0.5(1)	0.15(5)
Na ₂ O	2.52(4)	2.6(1)	2.47(9)	2.41(5)	2.58(8)
K ₂ O	0.075(9)	0.08(1)	0.12(1)	0.063(9)	0.10(2)
F	0.67(5)	0.6(1)	0.6(1)	0.7(2)	0.5(1)
H ₂ O	2.5(1)	2.5(1)	2.5(1)	2.4(1)	2.6(1)
Total	99.98	100.29	100.57	100.00	98.32
Number of cations calculated on the basis of 31 (O, OH, F)					
Si	5.86(6)	5.9(1)	5.83(7)	5.9(1)	5.92(8)
Ti ⁴⁺	0.005(2)	0.032(7)	0.003(3)	0.030(4)	0.002(1)
B	3	3	3	3	3
Al	2.06(5)	2.4(1)	2.91(8)	2.7(2)	3.33(9)
Cr ³⁺	4.41(6)	4.2(2)	3.37(8)	3.9(2)	3.2(1)
V ³⁺	0.36(3)	0.25(5)	0.82(7)	0.15(1)	0.36(4)
Fe ²⁺	0.048(9)	0.031(9)	0.02(1)	0.03(2)	0.03(1)
Mn ²⁺	–	–	–	–	–
Mg	2.24(3)	2.24(7)	2.05(7)	2.19(7)	2.14(4)
Zn	0.017(9)	0	0.007(7)	0.008(8)	0.012(7)
Ca	0.073(6)	0.07(2)	0.04(3)	0.10(2)	0.028(9)
Na	0.88(2)	0.89(4)	0.84(3)	0.83(2)	0.89(3)
K	0.017(2)	0.017(3)	0.027(3)	0.014(2)	0.022(5)
F	0.38(3)	0.33(7)	0.36(6)	0.4(1)	0.26(8)
OH	3.0(1)	3.0(1)	2.9(1)	2.8(1)	3.0(1)

Notes: Errors for oxides are the standard deviations of repeated analyses on the individual crystal. For B₂O₃ uncertainty was evaluated at 5%. Standard deviations for cations were calculated according to Wood and Virgo (1989).

exceed 0.4 apfu). The main divalent cation is Mg. The most striking feature of these crystals is the exceptionally high Cr content (from 3.2 to 4.41 apfu), which substitutes for Al, and, in sample TMt3b, reaches the highest value, so that all samples may be defined as belonging to the Cr-dravite–chromdravite subseries.

Determination of cation distribution

As already pointed out, cation distribution in tourmaline may be extremely complex, so that site assignment is not always straightforward. Several different procedures may be adopted to determine cation distribution, and very satisfactory results (*e.g.* Lavina *et al.*, 2002) may be obtained by combining data from EMPA (Electron MicroProbe Analysis), SREF (Structure REFinement) and MS (Mössbauer Spectroscopy).

This approach simultaneously takes into account both structural and chemical data and reproduces observed

parameters by optimising cation distribution. Differences between observed and calculated parameters are minimized using the “chi-square” function:

$$F(X_i) = \frac{1}{n} \sum_{j=1}^n \left(\frac{O_j - C_j(X_i)}{\sigma_j} \right)^2 \quad (1)$$

where O_j is observed quantity, σ_j its standard deviation, X_i variables, *i.e.*, cation fractions in tetrahedral and octahedral sites, and $C_j(X_i)$ the same quantity as O_j calculated by means of X_i parameters. The n O_j quantities taken into account were: unit cell parameters (a , c), O6 oxygen z coordinate (z_{O6}) and mean bond distances and m.a.n. of T , Y and Z sites, total atomic proportions given by microprobe analyses, and constraints imposed by crystal chemistry (total charges and T , Y and Z site populations).

Mean bond distances may be calculated as the linear contribution of each site cation (X_i) multiplied by its specific bond distance ($\langle T-O_i \rangle$, $\langle Y-O_i \rangle$ and $\langle Z-O_i \rangle$) according to:

$$\langle T-O \rangle_{\text{calc.}} = \sum X_i \langle T-O \rangle_i$$

$$\langle Y-O \rangle_{\text{calc.}} = \sum X_i \langle Y-O \rangle_i$$

$$\langle Z-O \rangle_{\text{calc.}} = \sum X_i \langle Z-O \rangle_i$$

In this way a , c and z_{O6} can be expressed as functions of $\langle T-O \rangle$, $\langle Y-O \rangle$ and $\langle Z-O \rangle$, the observed values of some selected bond distances and atomic coordinates. Full details of the minimization procedure may be found in Bosi & Lucchesi (2004). The T site was populated by Si and, subordinately, Al; Zn and Ti^{4+} , given their low quantities and following their general preference (Hawthorne, 1996; Hawthorne & Henry, 1999), were fixed in the Y site. As the X site was considered to be populated only by Na, K, Ca and vacancies, it was not included in the minimization procedure.

Optimal site assignment was executed by a quadratic program solver. Several minimization cycles of equation (1) up to convergence were performed using a home-developed calculation routine. Final $F(X_i)$ values ranging from 0.21 to 2.70 were obtained, confirming that almost all (> 96 %) chemical and structural parameters were reproduced, on average, within their experimental error (a table containing the differences between observed and calculated parameters may be obtained from the authors or through the E.J.M. Editorial Office - Paris); the corresponding site populations are collected in Table 6.

Empirical specific bond distances for ${}^YCr^{3+}-O$ and ${}^ZCr^{3+}-O$ (1.978 Å and 1.970 Å, respectively), valid for schorl–dravite–chromdravite samples, were optimised after a minimization procedure with the starting specific bond distances reported in Table 6.

Crystal chemistry

Site populations (Table 6) indicate that the crystals are characterized by quite disordered cation distribution between Y and Z octahedra. Cr^{3+} and Mg populate both

Table 6. Final assigned site population.

Sample	Tmt3b	Tmt6b	Tmt3c	TMpr79f	Tm1p43e
X site					
Na	0.880	0.892	0.842	0.829	0.888
Ca	0.073	0.068	0.043	0.097	0.028
K	0.017	0.017	0.027	0.014	0.022
Vacancy	0.030	0.022	0.087	0.060	0.062
Y site					
Ti^{4+}	0.004	0.029	0.002	0.030	0.002
Al	0.000	0.000	0.083	0.000	0.097
Cr^{3+}	2.132	2.229	1.740	2.298	2.174
V^{3+}	0.353	0.243	0.782	0.146	0.057
Fe^{2+}	0.051	0.036	0.021	0.042	0.001
Mg	0.439	0.462	0.363	0.473	0.651
Zn	0.021	0.000	0.008	0.011	0.016
ΣY	3.000	3.000	3.000	3.000	2.998
Z site					
Al	1.984	2.338	2.637	2.665	3.247
Cr^{3+}	2.211	1.799	1.634	1.600	0.971
V^{3+}	0.000	0.000	0.000	0.000	0.223
Fe^{2+}	0.002	0.000	0.006	0.000	0.038
Mg	1.803	1.863	1.722	1.734	1.519
ΣZ	5.999	6.000	6.000	6.000	5.998
T site					
Si	5.885	5.977	5.869	5.980	5.985
Al	0.113	0.022	0.130	0.020	0.012
ΣT	5.999	5.999	5.999	6.000	5.997
V site					
O^{2-}	0.000	0.018	0.064	0.179	0.000
OH	3.000	2.982	2.936	2.821	3.000
W site					
O^{2-}	0.609	0.668	0.639	0.607	0.707
OH	0.009	0.000	0.000	0.000	0.034
F	0.381	0.332	0.361	0.393	0.259

Notes: For all samples, B_3 and O_{27} .
 Specific bond distances - Å - optimised (Bosi and Lucchesi, 2004): Al = ${}^Y1.908 - {}^Z1.900$; $Cr^{3+} = {}^Y1.978 - {}^Z1.970$; $V^{3+} = {}^Y2.018 - {}^Z2.010$; $Fe^{2+} = {}^Y2.139 - {}^Z2.131$; Mg = ${}^Y2.084 - {}^Z2.077$; Si = ${}^Y1.619$.
 Specific bond distances - Å - calculated with Shannon's (1976) radii: $Ti^{4+} = {}^Y1.966$; Zn = ${}^Y2.101$; Al = ${}^Y1.975$.
 Uncertainty of specific bond distance was estimated ca. 0.001 Å.

sites but show opposite behaviour: Mg has a marked preference for the Z octahedron and Cr^{3+} for Y . Al almost exclusively populates the Z site and V^{3+} the Y site. This scheme follows the cation site preferences already observed in schorl–dravite – particularly for some Cr^{3+} -bearing (0.16–0.31 apfu) dravite samples (Bosi, 2001; Bosi & Lucchesi, 2004) – except for Mg, which shows the opposite behaviour. Intracrystalline disorder was also shown by the chromdravite refined by Gorskaya *et al.* (1984): $X(Na_{0.85}K_{0.07}Ca_{0.03}) {}^Y(Cr_{1.22}Fe_{1.03}Mg_{0.64}Mn_{0.06}Ti_{0.02}V_{0.01}) {}^Z(Cr_{3.90}Mg_{2.08}Al_{0.02}) B_3 Si_6 O_{27} (O_{1.14}OH_{2.86})$. This general behaviour is in line with the restrictions on Y and Z cation distribution imposed by the $OH^- \leftrightarrow O^{2-}$ substitution on W site (Hawthorne, 1996).

In the Cr–dravite–chromdravite subseries, most structural features are related to variations in Z (bond distances and polyhedral edges), whereas the dimensions of other polyhedra remain almost constant. As expected, in all samples Z polyhedral dimensions depend on site popula-

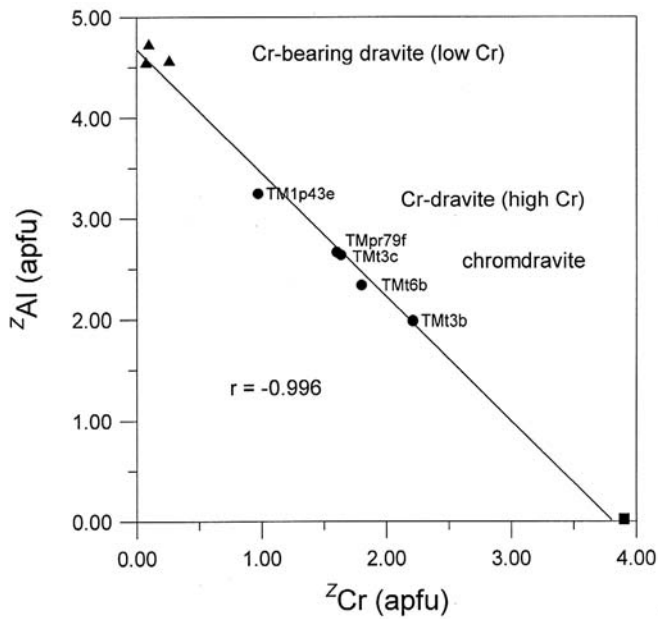


Fig. 2. Z site chemical variations in dravite–chromdravite series: $Z\text{Al} \leftrightarrow Z\text{Cr}^{3+}$. Full circles: Sludyanka samples; full square: chromdravite (Gorskaya *et al.*, 1984); full triangles: low-Cr dravites (Bosi, 2001; Bosi & Lucchesi, 2004). Regression line for all samples.

tions and, in particular, sample TMt3b (chromdravite) is characterized by the largest $\langle Z\text{-O} \rangle$ (1.979 Å), due to its lower content in $Z\text{Al}$ with respect to larger cations such as $Z\text{Mg}$ and $Z\text{Cr}^{3+}$ (Table 6). $Z\text{Cr}^{3+}$ ranges from 2.21 to 0.97 apfu, and is substituted essentially by $Z\text{Al}$, because $Z\text{Mg}$ is relatively constant (1.86–1.52 apfu). This behaviour is common also in the chromdravite studied by Gorskaya *et al.* (1984) and in the above described Cr-bearing dravites (Fig. 2). Z polyhedral distortion, $\langle \lambda_Z \rangle$, is larger – average value of 1.0151(1) – than in schorl–dravite samples (Bosi 2001; Bosi & Lucchesi, 2004; Bloodaxe *et al.*, 1999), for which an average value of $\langle \lambda_Z \rangle = 1.0139(5)$ was observed. Despite these differences are almost within the 2σ , they seem significant.

Y does not actively participate in structural variations, as $\langle Y\text{-O} \rangle$ (which ranges from 1.999 to 2.002 Å, reaching the highest value for chromdravite) does not show significant correlations with the single bond distances and polyhedral edges. The minimal dimensional variations are due to the cooperative effects of the various cations populating the site. Apart from the very minor contents of Ti^{4+} , Fe^{2+} and Zn, the Y site is dominated by Cr^{3+} (2.30–1.74 apfu), which is mainly substituted by V^{3+} (0.78–0.06 apfu). Also in this case, $Y\text{Mg}$ is quite constant (0.65–0.36 apfu). Because $Y\text{Cr}^{3+}$ and $Y\text{V}^{3+}$ dimensions are comparable and $Y\text{Al}$ content is minimal (< 0.10 apfu), the uniformity of Y polyhedral dimensions is easily justified. Unlike the case of Z, Y distortion, $\langle \lambda_Y \rangle$, decreases from Cr-dravite to chromdravite (1.0194 – 1.0180), in line with the inverse correlation ($r = -0.90$) between $\langle Z\text{-O} \rangle$ and $\langle \lambda_Y \rangle$ observed in schorl–dravite samples (Bloodaxe *et al.*, 1999; Bosi, 2001; Bosi & Lucchesi, 2004). The same considerations also apply to the $\langle Y\text{-O} \rangle$ and $\langle \lambda_Z \rangle$ correlation: Z distortion is

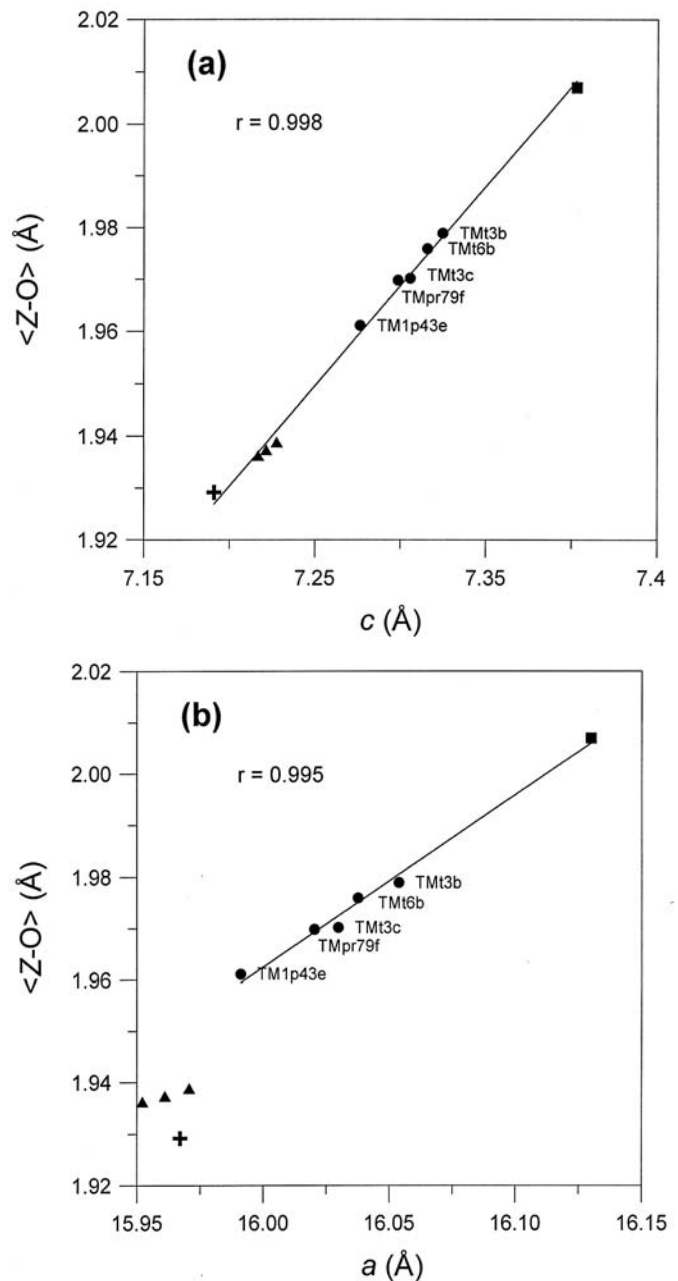


Fig. 3. Variations of structural parameters in dravite–chromdravite series. Full circles: Sludyanka samples; full square: chromdravite (Gorskaya *et al.*, 1984); full triangles: low-Cr dravites (Bosi, 2001; Bosi & Lucchesi, 2004); cross: low-Cr V-dravite (Foit & Rosenberg, 1979). (a) $\langle Z\text{-O} \rangle$ vs. c . Regression line for all samples. (b) $\langle Z\text{-O} \rangle$ vs. a . Regression line only for chromdravite samples.

almost constant, because Y volume variation is minimal. As Y and Z interact by the O3–O6 edge, the latter is correlated only to $\langle Z\text{-O} \rangle$ and not to $\langle Y\text{-O} \rangle$, as observed in the schorl–dravite series.

T is characterized by low $T\text{Al}$ contents (0.01–0.13 apfu), which are responsible for the slightly larger dimensions ($\langle T\text{-O} \rangle$ from 1.618 to 1.621 Å) compared with 1.616 Å, values characteristic of full tetrahedral Si occupancy in

tourmaline (Hawthorne, 1996); see also Table 6 for comparison.

X is almost totally populated by Na (0.83–0.89 apfu) and this compositional constancy is reflected in its dimensions which are almost identical among samples (Table 4), within the limits of experimental uncertainty. The same holds for the B site, whose chemical contents were fixed to full B occupancy, on the basis of the considerations listed above.

In the dravite–chromdravite series, the unit cell parameter c is strongly and positively correlated with Z dimensions (Fig. 3a) whereas a positive a vs. $\langle Z-O \rangle$ correlation is evident only within the Cr-dravite–chromdravite subseries (Fig. 3b). No significant correlation was observed between Y dimensions and unit cell parameters.

Concluding, and differently from the schorl–dravite series (Bosi, 2001; Bosi & Lucchesi, 2004), most structural variations are thus due to Z , whereas the effects of Y are negligible. This behaviour stands out when examining the a vs. c plot (Fig. 4) in the whole series. A strong correlation ($c = 0.9226a - 7.4809$; $r = 0.997$) between the two unit cell parameters was obtained in the Cr-dravite–chromdravite subseries, but the dravite samples collected from the literature plot over a large area and, in particular, the Cr-bearing dravite samples (low-Cr) do not lie on the regression line.

Acknowledgements: This work was supported by MURST and RFBR (Russian Foundation for Basic Research, projects 01-05-97234 and 02-05-69329) grants.

References

- Barton, R., Jr. (1969): Refinement of the crystal structure of buergerite and the absolute orientation of tourmalines. *Acta Cryst.*, **B25**, 1524–1533.
- Bosi, F. (2001): Crystal-chemistry of the minerals of the tourmaline group. 176 p. Ph.D. dissertation, University of Rome “La Sapienza”, Rome (in Italian).
- Bosi, F. & Lucchesi, S. (2004): Crystal chemistry of the schorl–dravite series. *Eur. J. Mineral.*, **16**, 335–344.
- Bloodaxe, E.S., Hughes, J.M., Dyar, M.D., Grew, E.S., Guidotti, C.V. (1999): Linking structure and chemistry in the schorl–dravite series. *Am. Mineral.*, **84**, 922–928.
- Cossa, A. & Arzruni, A. (1883): Chromtourmalin aus den Chromeisenlagern des Ural. *Zeit. für Krystall. Mineral.*, **7**, 1.
- Foit, F.F., Jr. (1989): Crystal chemistry of alkali-deficient schorl and tourmaline structural relationships. *Am. Mineral.*, **74**, 422–431.
- Foit, F.F., Jr. & Rosenberg, P.E. (1979): The structure of vanadium-bearing tourmaline and its implications regarding tourmaline solid solutions. *Am. Mineral.*, **64**, 788–798.
- Gorskaya, M.G., Frank-Kamenetskaya, O.V., Rozhdestvenskaya, I.V. Frank-Kamenetskii, V.A. (1984): Crystal structure of chromdravite, a new mineral. *Proceedings 27th International Geological Congress, Moscow, Russia*, 48–49.
- Hawthorne, F.C. (1996): Structural mechanisms for light-element variations in tourmaline. *Can. Mineral.*, **34**, 123–132.
- Hawthorne, F.C. & Henry, D. (1999): Classification of the minerals of the tourmaline group. *Eur. J. Mineral.*, **11**, 201–215.
- Hawthorne, F.C., Burns, P.C., Grice, J.D. (1996): The crystal chemistry of boron. In “Boron: Mineralogy, Petrology and Geochemistry, Reviews in Mineralogy, 33”, L.M. Anovitz & E.S. Grew, eds. Mineralogical Society of America, 41–115.
- Hughes, K.A., Hughes, J.M., Dyar, M.D. (2001): Chemical and structural evidence for $^{41}\text{B} \leftrightarrow ^{41}\text{Si}$ substitution in natural tourmalines. *Eur. J. Mineral.*, **13**, 743–747.
- Lavina, B., Salviulo, G., Della Giusta, A. (2002): Cation distribution and structure modelling of spinel solid solutions. *Phys. Chem. Minerals*, **29**, 10–18.
- MacDonald, D.J. & Hawthorne, F.C. (1995): The crystal chemistry of Si \leftrightarrow Al substitution in tourmaline. *Can. Mineral.*, **33**, 849–858.
- Nuber, B. & Schmetzer, K. (1979): Die Gitterposition des Cr^{3+} im Turmalin: Strukturverfeinerung eines Cr-reichen Mg-Al-Tourmalins. *N. Jb. für Mineral. Abh.*, **137**, 184–197.
- Pieczka, A. (1999): Statistical interpretation of structural parameters of tourmalines: the ordering of ions in the octahedral sites. *Eur. J. Mineral.*, **11**, 243–251.
- Pouchou, J.L. & Pichoir, F. (1984): A new model for quantitative X-ray micro-analysis. I. Application to the analysis of homogeneous samples. *La Recherche Aérospatiale*, **3**, 13–36.
- Reznitskii, L.Z. & Sklyarov, E.V. (1996): Unique Cr–V mineral association in metacarbonate rocks of the Sludyanka, Russia. *Proceedings 30th International Geological Congress, Beijing, China*, 446.
- Reznitskii, L.Z., Sklyarov, E.V., Ushapovskaya, Z.F. (1988): Minerals of chromium and vanadium in Sludyanka Crystalline Complex (southern Pribaikalia). In “Metamorphic formations of Pre-Cambrian of Eastern Siberia”, V.G. Belichenko, ed. Nauka, Novosibirsk, Russia, p. 64–74.
- Reznitskii, L.Z., Sklyarov, E.V., Ushapovskaya, Z.F., Nartova, N.V., Evsyunin, V.G., Kashaev, A.A., and Suvorova, L.F. (1997):

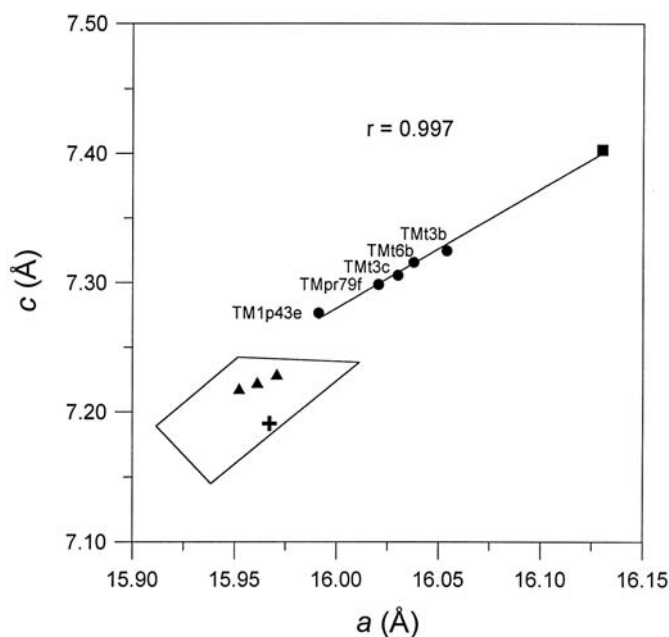


Fig. 4. Dravite–chromdravite series: c vs. a . Outlined polygon shows area in which “dravite” samples from literature plot (Bosi, 2001; Bosi & Lucchesi, 2004; Bloodaxe *et al.*, 1999; Foit & Rosenberg, 1979). Full circles: Sludyanka samples; full square: chromdravite (Gorskaya *et al.*, 1984); full triangles: low-Cr dravites (Bosi, 2001; Bosi & Lucchesi, 2004); cross: low-Cr V-dravite (Foit & Rosenberg, 1979).

- Chromphyllite $\text{KCr}_2[\text{AlSi}_3\text{O}_{10}](\text{OH}, \text{F})_2$ – a new dioctahedral mica. *Proc. Russian Mineral. Soc.*, **126**, 110-119.
- Reznitskii, L.Z., Sklyarov, E.V., Ushchapovskaya, Z.F., Nartova, N.V., Kashaev, A.A., Karmanov, N.S., Kanakin, S.V., Smolin, A.S., Nekrasova, E.A. (2001): Vanadiumdravite $\text{NaMg}_3\text{V}_6[\text{Si}_6\text{O}_{18}][\text{BO}_3]_3(\text{OH})_4$, a new mineral of the tourmaline group. *Proc. Russian Mineral. Soc.*, **130**, 59-72.
- Robinson, K., Gibbs G.V., Ribbe, P.H. (1971): Quadratic elongation: A quantitative measure of distortion in coordination polyhedra. *Science*, **172**, 567-570.
- Rumyantseva, E.V. (1983): Chromdravite, a new mineral from Karelia. *Proc. Russian Mineral. Soc.*, **112**, 222-225.
- Salnikova, E.B., Sergeev, S.A., Kotov, A.B., Yakovleva, S.Z., Steiger, R.H., Reznitskii, L.Z., Vasil'ev, E.P. (1998): U-Pb zircon dating of granulite metamorphism in the Sludyanskiy Complex, Eastern Siberia. *Gondwana Res.*, **1**, 195-205.
- Shannon, R.D. (1976): Revised effective ionic radii and systematic studies of interatomic distances in halides and chalcogenides. *Acta Cryst.*, **A32**, 751-767.
- Wood, B.J. & Virgo, D. (1989): Upper mantle oxidation state: Ferric iron contents of lherzolite spinels by ^{57}Fe Mössbauer spectroscopy and resultant oxygen fugacity. *Geochim. Cosmochim. Acta*, **53**, 1277-1291.

Received 22 May 2003

Modified version received 25 September 2003

Accepted 27 November 2003